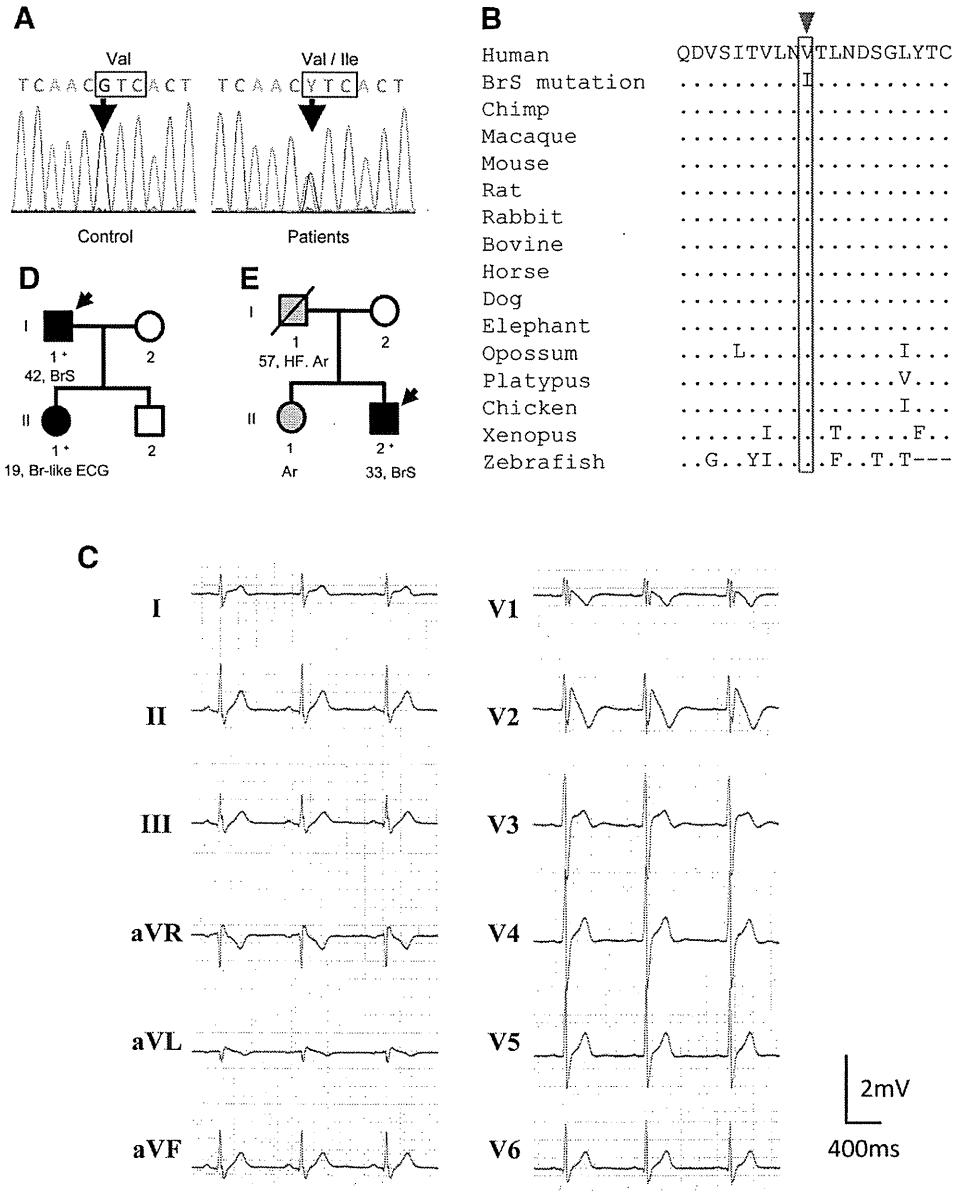


**Figure 1.** Mutational analysis of *SCN3B* in Brugada syndrome (BrS). (**A**) Direct sequencing analysis of exon 3 in a control (**Left**) and a patient, BrS-H-1 (**Right**), shows that the patient was heterozygous for GTC and ATC (Ile) at codon 110, where the control was homozygous for GTC (Val). The same pattern was obtained from the other proband patients, BrS-O-1 and BrS-S-1, as well as from BrS-O-2 who was a daughter of BrS-O-1 (**Table 1**). (**B**) Amino acid sequences of Nav$\beta$3 from various species aligned with the V110I mutation. (**C**) Representative ECG recording from BrS-O-1 shows typical coved-type ST-segment elevation in leads V1–2. Pedigrees of BrS families with the V110I mutation: BrS-O-1 (**D**) and BrS-S-1 (**E**). Squares and circles indicate male and female, respectively. Filled and open symbols represent affected and unaffected individuals, respectively. Shaded symbols indicate subjects with undefined arrhythmia (Ar). Arrows indicate the proband patients. Presence of the mutation is noted as +. Ages at blood sampling or death are indicated. HF, heart failure.

encoding modifier proteins of Nav1.5, which causes functional loss of $I_{Na}$.[8,12,22–25] Among the modifier proteins, Nav$\beta$3, which does not form the ion-conducting pore, modifies the function of Nav1.5 by modulating channel gating and increasing the cell surface expression of Nav1.5,[26] and hence *SCN3B* mutations could be responsible for BrS. Nevertheless, there is only 1 report of a *SCN3B* mutation, Leu10Pro, in an American patient with BrS,[23] although some other *SCN3B* mutations have been reported in other hereditary arrhythmias, including IVF,[27] SIDS,[28] and AF.[29,30]

We report a *SCN3B* mutation, Val110Ile, found in 3 unrelated Japanese BrS patients. Functional studies in transfected cells demonstrated that the mutation decreased the cell surface expression of Nav1.5 and reduced the peak current of the $I_{Na}$.

**Table 1. Clinical Phenotypes of Individuals Carrying the *SCN3B* Val110Ile Mutation**

| ID | Age (years)/Sex | ST-elevation type | Symptoms | Family history of arrhythmia/SCD | ICD | EPS |
|---|---|---|---|---|---|---|
| BrS-O-1 | 42/M | Coved | Symptomatic | Yes | Yes | VF |
| BrS-O-2 | 19/F | Coved | Asymptomatic | Yes | No | – |
| BrS-S-1 | 33/M | Saddleback | Asymptomatic | Yes | No | NSVT |
| BrS-H-1 | 51/M | Coved | Syncope | No | No | – |

BrS, Brugada syndrome; EPS, electrophysiologic study; ICD, implantable cardioverter defibrillator; NSVT, non-sustained ventricular tachycardia; SCD, sudden cardiac death; VF, ventricular fibrillation.

## Methods

### Subjects

We studied 178 genetically unrelated Japanese and 3 Korean patients with BrS. Age at the diagnosis of 145 male patients was 45.3±15.7 (range 7–76) years, and that of the 17 female patients was 46.8±17.3 (range 11–72) years. Episodes of syncope and/or arrhythmia had occurred in 93 patients, but the others were asymptomatic. There was a family history of sudden death and/or arrhythmias for 19 patients, but nothing certain for the others. Blood samples were obtained from each subject after informed consent for gene analysis was given. The patients had been analyzed for mutations in *SCN5A* by using specific primer pairs (**Table S1**), and no disease-related mutation was found. The control subjects were 480 genetically unrelated Japanese individuals who were selected at random without ECG records.

The research protocol was approved by the Ethics Review Committee of the Medical Research Institute, Tokyo Medical and Dental University and the Institutional Review Board of Samsung Medical Center.

### Mutational Analysis

Genomic DNA extracted from the peripheral blood leukocytes of each individual was subjected to polymerase chain reaction (PCR) using primer pairs specific to *SCN3B* (**Table S2**). PCR products were analyzed for mutations by direct DNA sequencing using Big Dye Terminator version 3.1 and ABI3100 DNA analyzer (Applied Biosystems, Foster City, CA, USA). The proband patients carrying the Val110Ile mutation were analyzed for mutations in the other known BrS susceptibility genes, *CACNA1C*, *CACNB2*, *GPD1-L*, *KCNJ8*, *SCN1B*, *KCNE3*, *MOG1*, *HCN4*, *KCND3* and *KCNE5*, by sequencing of PCR products amplified with specific primer pairs (**Table S1**).

### Alignment of Amino Acid Sequences

Amino acid sequences of human Nav$\beta$3 protein predicted from the nucleotide sequences (GenBank™ NM_018400) were aligned with those of chimpanzee (XM_522210), macaque (NM_001194283), mouse (NM_153522), rat (NM_139097), rabbit (ENSOCUP00000009050), bovine (NM_001046495), horse (ENSECAT00000025763), dog (XM_847682), elephant (ENSLAFT00000000307), opossum (XM_001379934), platypus (ENSOANT00000023925), chicken (XM_417884), *Xenopus* (NM_001011299), and zebrafish (NM_001080802).

### Constructs for Nav1.5 and Nav$\beta$3

We obtained a cDNA fragment of human Nav$\beta$3 by reverse transcription-PCR from human adult heart cDNA. Mutant cDNA fragments of Nav$\beta$3 containing a T to C substitution in codon 10 (for Leu10Pro mutation) or a G to A substitution at codon 110 (for Val110Ile mutation) were created by the primer-mediated mutagenesis method using specific primers (**Table S3**). Wild-type (WT) or mutant cDNA fragments were cloned into pcDNA3.1-myc, His-B (myc-His-Nav$\beta$3) (Invitrogen, San Diego, CA, USA) and pIRES-CD8 (pIRES-CD8-Nav$\beta$3). The cDNA fragment of human *SCN5A* was a gift from Dr A.L. George (Vanderbilt University). A Flag-tagged Nav1.5 was constructed by inserting a Flag epitope (DYKDDDDK) into the extracellular linker 1 (L1) between S1 and S2 in the D1 domain after position aa154 in the Nav1.5 construct (L1-Flag-Nav1.5), as described previously.[18] All constructs were sequenced to ensure that no errors were introduced.

### Immunofluorescence Microscopy

We seeded $4.0\times10^4$ tsA-201 cells, a derivative line of HEK cells, onto poly-D-Lysine 8-well culture slides (BD Biosciences, San Jose, CA, USA), and 24 h later, myc-His-Nav$\beta$3 (0.1 $\mu$g) alone, or L1-Flag-Nav1.5 (0.1 $\mu$g) plus myc-His-Nav$\beta$3 (0.1 $\mu$g) were added to the wells with Lipofectamine 2000 Reagent (Invitrogen) (0.2 or 0.4 $\mu$l, respectively). After 18 h, the cells were washed with phosphate-buffered saline (PBS), fixed in 4% paraformaldehyde for 15 min at room temperature and permeabilized by 0.15% Triton X-100 in PBS with 3% bovine serum for 20 min at room temperature. The cells were then incubated with the primary rabbit anti-Flag polyclonal antibody (Ab) (1:250, Sigma, CA, USA) and mouse anti-myc monoclonal Ab (1:200, Santa Cruz Biotechnology, Santa Cruz, CA, USA), and secondary Alexa Fluor 568 goat anti-rabbit IgG (1:500, Molecular Probes, Eugene, OR, USA) and Alexa Fluor 488 rabbit anti-mouse IgG (1:1,000, Molecular Probes), respectively, in PBS with 3% bovine serum. All cells were mounted on glass slides using Mowiol 4-88 Reagent (Calbiochem, Darmstadt, Germany), and images were collected and analyzed with an LSM510 laser-scanning microscope (Carl Zeiss Microscopy, Jena, Germany). To quantify the membrane expression of Nav1.5, fluorescence intensity of the total cell and the plasma membrane (peripheral, 2 $\mu$m) areas in the middle *xy* images of *z* series stack were measured, and the ratios of peripheral to total cell area fluorescence intensity (PTAFI) were calculated as described previously.[23] Analyses of labeled cells were performed using ImageJ software (NIH, MD, USA).[31]

### Electrophysiological Studies

The tsA-201 cell line was used in the electrophysiological study, as described previously.[18] Cells transfected with pIRES-CD8 or pIRES-CD8-Nav$\beta$3 were briefly preincubated with Dynabeads M-450 CD8 (Dynal, Oslo, Norway) prior to the recordings. Sodium currents were recorded from the cells that were labeled with Dynabeads using the whole-cell patch clamp technique. Currents and cell capacitances were recorded using Axopatch 200B amplifier (Axon Instruments, CA, USA) and series resistance errors were reduced by 60–70% using elec-

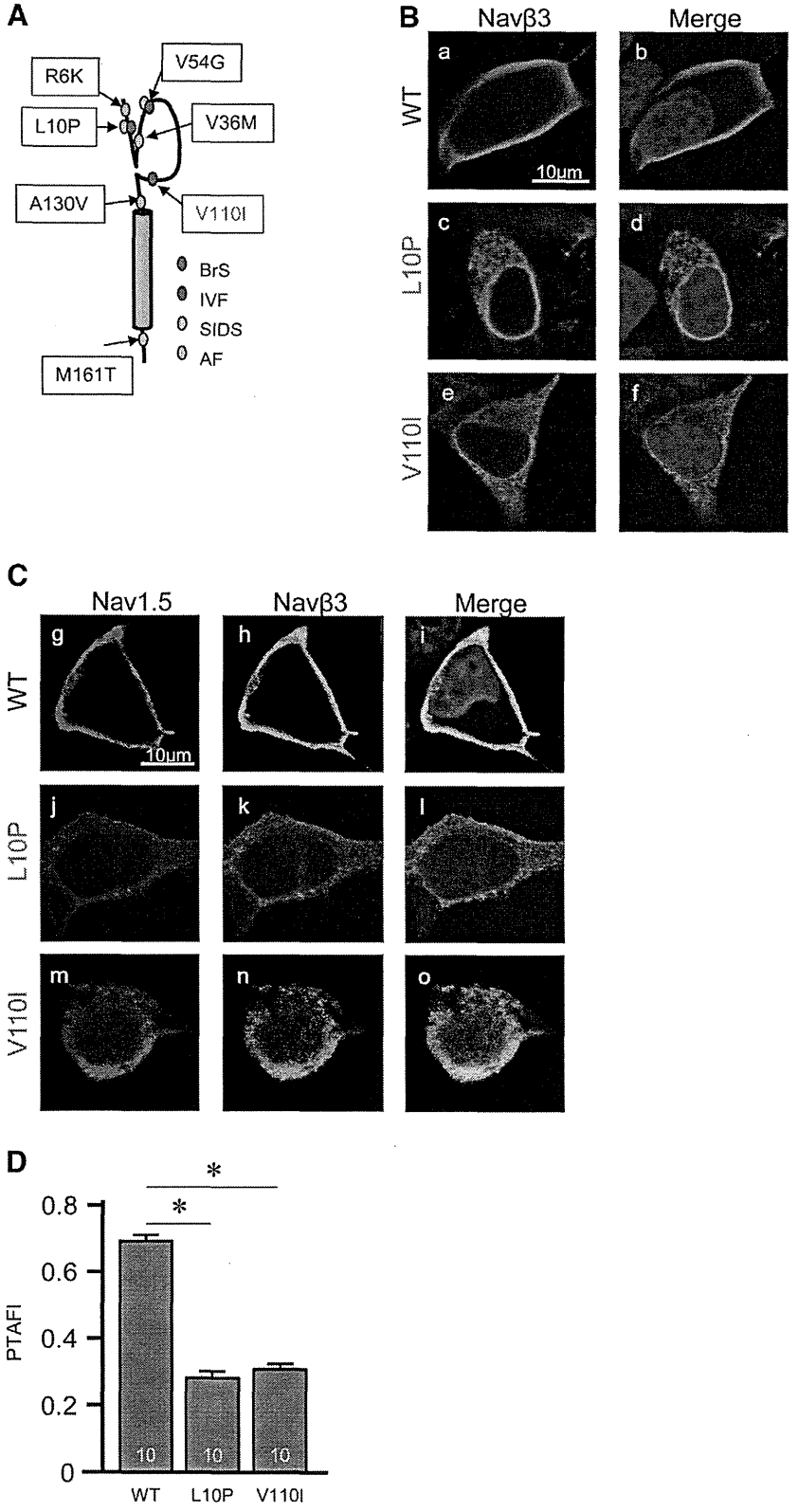


**Figure 2.** *SCN3B* mutations reported in arrhythmias and distribution of Nav1.5 and Navβ3 in transfected tsA-201 cells. (**A**) Schematic representation of Navβ3 mutations found in arrhythmias. *SCN3B* mutations in BrS (red), IVF (purple), SIDS (light green), and AF (light blue) are mapped on the Navβ3. Extracellular domain and transmembrane domain are indicated. The V110I mutation found in this study is indicated in red. (**B**,**C**) tsA-201 cells transfected with myc-His-Navβ3-WT (**a**,**b**), -L10P (**c**,**d**) or -V110I (**e**,**f**), and the combination of L1-Flag-Nav1.5 and myc-His-Navβ3-WT (**g**–**i**), -L10P (**j**–**l**), or -V110I (**m**–**o**). The cells were permeabilized by 0.15% Triton X-100 and stained with anti-myc Ab (Navβ3, green; **a**,**c**,**e**,**h**,**k**,**n**) and anti-Flag Ab (Nav1.5, red; **g**,**j**,**m**). Nuclei were stained with DAPI and merged images are shown in **b**,**d**,**f**,**i**,**l**, and **o**. Scale bar=10 μm. (**D**) The ratio of peripheral to total cell area fluorescence intensity (PTAFI) of expressed L1-Flag-hNav1.5 in the transfected cells. Numbers of analyzed cells are indicated at the bottom of each bar. Data are expressed as mean± SEM. *P<0.001. AF, atrial fibrillation; BrS, Brugada syndrome; IVF, idiopathic ventricular fibrillation; SIDS, sudden infant death syndrome.

**Table 2. Kinetics of $I_{Na}$ in Transfected tsA-201 Cells**

| Transfected constructs | Peak $I_{Na}$ (at −25 mV) | | Activation | | | Inactivation | | | Recovery | |
|---|---|---|---|---|---|---|---|---|---|---|
| | pA/pF | n | $V_{1/2}$ (mV) | $\kappa$ | n | $V_{1/2}$ (mV) | $\kappa$ | n | Time required for $e^{-1}$ fraction recovery (ms) | n |
| SCN5A without SCN3B | −59.83±11.36** | 10 | −35.23±1.83* | −7.49±0.29* | 10 | −78.66±1.59* | 7.63±0.29* | 10 | 10.29±0.81** | 9 |
| SCN5A+SCN3B-WT | −110.28±8.92 | 11 | −43.22±2.11 | −6.68±0.21 | 11 | −82.40±1.96 | 6.83±0.15 | 11 | 6.06±1.10 | 9 |
| SCN5A+SCN3B-L10P | −68.09±5.81** | 13 | −40.39±1.98 | −6.51±0.17 | 13 | −83.49±1.10 | 6.40±0.23 | 11 | 8.88±0.99** | 10 |
| SCN5A+SCN3B-V110I | −62.72±5.10** | 15 | −40.28±1.82 | −6.35±0.12 | 15 | −81.98±1.34 | 6.60±0.18 | 15 | 6.10±0.92 | 12 |
| SCN5A+SCN3B-WT/L10P | −82.46±8.21* | 13 | −41.49±2.01 | −6.27±0.19 | 13 | −81.76±1.49 | 6.59±0.27 | 13 | 6.87±1.00 | 12 |
| SCN5A+SCN3B-WT/V110I | −77.77±7.31** | 13 | −41.57±1.45 | −6.16±0.26 | 13 | −81.17±1.03 | 6.44±0.13 | 12 | 6.44±1.45 | 12 |

*P<0.05 vs. SCN5A+SCN3B-WT, **P<0.01 vs. SCN5A+SCN3B-WT.
$I_{Na}$, inward sodium current; WT, wild-type.

tronic compensation. Holding potentials were −120 mV and pipette resistance was 1.0–1.5MΩ. The bath solution contained 36 mmol/L NaCl, 109 mmol/L NMG, 4 mmol/L KCl, 1.8 mmol/L $CaCl_2$, 1 mmol/L $MgCl_2$, and 10 mmol/L HEPES, pH 7.35, while the pipette solution contained 10 mmol/L NaF,110 mmol/L CsF, 20 mmol/L CsCl, 10 mmol/L EGTA, and 10 mmol/L HEPES, pH 7.35. All signals were acquired at 20–50 kHz (Digidata 1332, Axon Instruments) with a personal computer running Clampex 8 software (Axon Instruments) and filtered at 5 kHz with a 4-pole Bessel low-pass filter. Experiments were done at room temperature. Membrane currents were analyzed with Clampfit 8 software (Axon Instruments) and Sigmaplot (Systat Software, CA, USA). The current-voltage relationships were fit to the Boltzmann equation,

$$I=(V-V_{rev})\times G_{max}\times[1+\exp(V-V_{1/2})/\kappa]-1,$$

where $I$ is the peak sodium current during the test pulse potential $V$. The parameters estimated by the fitting are $V_{rev}$ (reversal potential), $G_{max}$ (maximum conductance), and $\kappa$ (slope factor). Steady-state availability was fit with the Boltzmann equation,

$$I/I_{max}=[1+\exp((V-V_{1/2})/\kappa)]-1,$$

where $I_{max}$ is the maximum peak sodium current, to determine the membrane potential for $V_{1/2}$ (half-maximal inactivation) and $\kappa$ (slope factor). The time course of inactivation was fit with a 2-exponential function,

$$I(t)/I_{max}=A0+A1\times\exp(-t/\tau_1)+A2\times\exp(-t/\tau_2),$$

where A and $\tau$ are amplitudes and time constants, respectively. $I$ and $t$ refer to current and time, respectively.

### Co-Immunoprecipitation (co-IP) Assay

The tsA-201 cells were transiently transfected with a combination of L1-Flag-Nav1.5 (2 μg) and myc-His-Navβ3 (2 μg). Cellular extracts were prepared from the transfected cells and equal amount of extracted proteins were used for the co-IP assay using the Catch and Release version 2.0 reversible immunoprecipitation system, according to the manufacturer's instructions (Millipore, Milford, MA, USA), with rabbit anti-Flag polyclonal Ab (Sigma). Eluted samples were separated by SDS-PAGE, transferred to a nitrocellulose membrane, pre-incubated with 5% skimmed milk in PBS, and incubated with primary mouse anti-c-myc monoclonal Ab (1:100) followed by secondary rabbit anti-mouse (for monoclonal Ab) IgG HRP-conjugated Ab (1:1,000; Dako A/S, Glostrup, Denmark).

### Statistical Analysis

Numerical data are expressed as mean±SEM. Statistical differences were analyzed using 1-way analysis of variance (ANOVA) followed by Dunnett's test. P<0.05 was considered to be statistically significant.

## Results

### Mutational Analysis of SCN3B

We analyzed 181 BrS patients, who were negative for *SCN5A* mutations, for sequence variations in *SCN3B* and found a synonymous and another non-synonymous variant in 1 and 3 patients, respectively. The synonymous variant, p.Asn113Asn (c.339C>T), was rare and was not considered to be a disease-causing mutation because no functional effect was deduced. On the other hand, the non-synonymous variant, p.Val110Ile (V110I, c.328G>A) (**Figure 1A**), was found in 3 unrelated Japanese patients; a 42-year-old male (BrS-O-1), a 33-year-old male (BrS-S-1), and a 51-year-old male (BrS-H-1) (**Table 1**). The V110I variant was predicted to affect an evolutionary conserved residue of Navβ3 (**Figure 1B**) and was not found in 960 control chromosomes. As summarized in **Table 1**, BrS-O-1 had experienced repetitive syncope, and showed spontaneous coved-type ST-elevation in ECG (**Figure 1C**). His daughter (BrS-O-2) was asymptomatic, but exhibited a BrS-like ECG pattern and carried the same mutation (**Table 1, Figure 1D**). BrS-S-1 was asymptomatic, showed saddleback-type ST-segment elevation, and pilsicainide administration converted the ST-segment elevation into the coved type. His father and sister had arrhythmia, although the details could not be evaluated (**Figure 1E**). BrS-H-1 had experienced syncope, and showed spontaneous coved-type ST-elevation in ECG, but the family history of arrhythmia was uncertain. These 3 proband patients were also analyzed for mutations in the other known disease genes for BrS (**Table S1**) and none had any mutation.

### Cell Surface Expression of Nav1.5 in the Presence of Mutant Navβ3

Navβ3 modulates the function of the Nav1.5 channel, and several *SCN3B* mutations have been reported in association with arrhythmias, including BrS, IVF, SIDS, and AF (**Figure 2A**). Because the Leu10Pro (L10P) mutation was the only mutation previously reported in only 1 BrS patient, which resulted in the reduction of $I_{Na}$ in transfected cells,[23] we investigated the functional alterations caused by the V110I mutation as compared with the L10P mutation. Membrane surface expression of Nav1.5 was examined in tsA-201 cells transfected with myc-His-Navβ3 alone or in combination with L1-Flag-Nav1.5. It was observed that Navβ3-WT was expressed on the cell

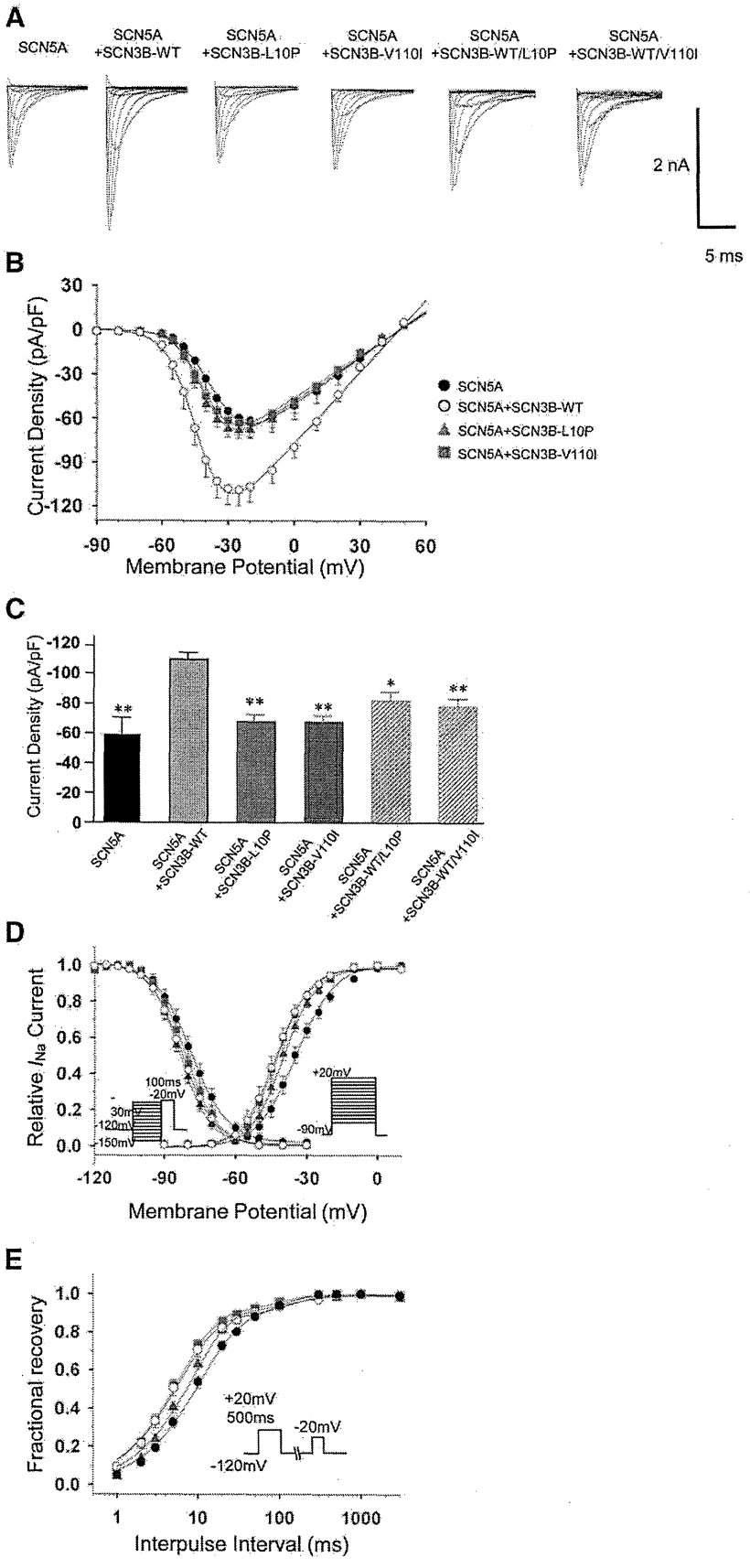


***Figure 3.*** Electrophysiological profiles of sodium currents recorded from tsA-201 cells transiently expressing Nav1.5 and Nav$\beta$3. (**A**) Representative sodium currents recorded from tsA-201 cells cotransfected with pcDNA3.1-Nav1.5 and pIRES-CD8 or pIRES-CD8-Nav$\beta$3. The traces were recorded with a whole-cell configuration. (**B**) Current-voltage relationship for peak $I_{Na}$. (**C**) Sodium current density at –25mV. Co-expression of Nav1.5 and Nav$\beta$3-WT increased the peak current densities by 83.9%, as compared with Nav1.5 alone, while co-expression of Nav1.5 with Nav$\beta$3-L10P or -V110I showed significantly smaller peak current densities than co-expression of Nav1.5 with Nav$\beta$3-WT by 37.5% and 42.5%, respectively (n=11 for WT, n=13 for L10P, n=15 for V110I). Co-expression of Nav1.5 and Nav$\beta$3-WT plus -L10P or -V110I also showed significantly smaller peak current densities than co-expression of Nav1.5 and Nav$\beta$3-WT by 25.2% or 29.4%, respectively (n=13 for WT/L10P, n=13 for WT/V110I). (**D**) Transfected cells of pcDNA3.1-Nav1.5 and pIRES-CD8-Nav$\beta$3-WT show a leftward shift in the voltage dependence of steady-state fast inactivation and activation, compared with transfected cells of pcDNA3.1-Nav1.5 and pIRES-CD8. Voltage dependences recorded from the transfected cells of pcDNA3.1-Nav1.5 in combination with pIRES-CD8-Nav$\beta$3-L10P, or -V110I were similar to that from the cells cotransfected with pcDNA3.1-Nav1.5 and pIRES-CD8-Nav$\beta$3-WT. (**E**) Transfected cells of pcDNA3.1-Nav1.5 and pIRES-CD8-Nav$\beta$3-WT show a leftward shift in the recovery from inactivation assessed by the double-pulse protocol, compared with transfected cells of pcDNA3.1-Nav1.5 and pIRES-CD8. Recovery from inactivation was nearly identical among Nav$\beta$3-WT, and -V110I, whereas L10P showed a significant rightward shift. The 2-pulse protocol is shown in the inset. WT, wild-type.

surface, whereas both Navβ3-L10P and Navβ3-V110I were retained in the cytoplasm (**Figures 2B-a–f**). In the cells co-transfected with Nav1.5 and myc-His-Navβ3, Nav1.5 was clearly expressed on the cell surface in the presence of Navβ3-WT (**Figures 2C-g–i**), but its cytoplasmic trafficking was disturbed by both Navβ3-L10P and Navβ3-V110I (**Figures 2C-j–o**). To express the trafficking defects quantitatively, we measured the fluorescence intensity of Nav1.5 in both the plasma membrane region and the entire cell area to obtain the ratios of PTAFI. As shown in **Figure 2D**, both the L10P and V110I mutation of *SCN3B* significantly reduced the cell surface expression of Nav1.5 by approximately 70%.

### Altered Electrophysiological Characteristics of $I_{Na}$ Caused by the *SCN3B* Mutations

Because the V110I mutation impaired the intracellular trafficking of Nav1.5, we investigated the potential effect of V110I mutation on Nav1.5 kinetics. Whole-cell patch clamp recordings were obtained from tsA-201 cells transiently transfected with pcDNA3.1-Nav1.5 in combination with pIRES-CD8, pIRES-CD8-Navβ3-WT, -L10P or -V110I (**Figure 3, Table 2**). It was found that the peak current densities of $I_{Na}$ from the cells cotransfected with pcDNA3.1-Nav1.5 and pIRES-CD8-Navβ3-WT were significantly larger than that recorded from the cells cotransfected with pcDNA3.1-Nav1.5 and pIRES-CD8 by 83.9% (**Figures 3B,C, Table 2**). However, the peak current densities of $I_{Na}$ recorded from the cells co-transfected with pcDNA3.1-Nav1.5 and pIRES-CD8-Navβ3-L10P or -V110I were significantly smaller than that recorded from the cells cotransfected with pcDNA3.1-Nav1.5 and pIRES-CD8-Navβ3-WT by 37.5% or 42.5%, respectively (**Figures 3B,C, Table 2**).

It also was observed that pIRES-CD8-Navβ3-WT shifted the voltage dependence of activation and inactivation to more negative potentials compared with pIRES-CD8, and neither pIRES-CD8-Navβ3-L10P nor -V110I caused any significant changes in the activation and inactivation kinetics of $I_{Na}$ compared with pIRES-CD8-Navβ3-WT (**Figure 3D, Table 2**). In accordance with the previous report,[23] pIRES-CD8-Navβ3-L10P caused a rightward shift in the time course of recovery from inactivation, whereas pIRES-CD8-Navβ3-V110I did not show any significant changes (**Figure 3E, Table 2**). To analyze the functional impact of mutant Navβ3 in the heterozygous state, the sodium current was recorded from cells expressing Nav1.5 in combination with WT and mutant Navβ3. It was demonstrated that the peak current densities of $I_{Na}$ recorded from the pcDNA3.1-Nav1.5-transected cells with pIRES-CD8-Navβ3-WT+L10P or -WT+V110I were significantly smaller than that from the transfected cells with pIRES-CD8-Navβ3-WT by 25.2% or 29.4%, respectively (**Table 2**). These data indicated that neither mutation exerted a dominant negative effect on the function of normal Navβ3.

### Binding Between Nav1.5 and Navβ3

Because Navβ3 non-covalently interacts with Nav1.5, we investigated whether the V110I mutation would change the interaction, but there were no significant differences among Navβ3-WT, -L10P and -V110I in binding Nav1.5 (**Figure 4**), indicating that the altered sodium channel function was not caused by loss of binding between Nav1.5 and Navβ3.

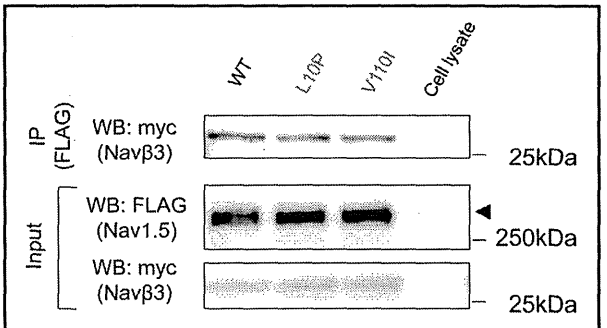


**Figure 4.** Binding assay between Navβ3 and Nav1.5. The tsA-201 cells were cotransfected with Flag-tagged Nav1.5 (L1-Flag-Nav1.5) and myc-tagged Navβ3 (myc-His-Navβ3) of WT, L10P or V110I. Cell lysates were prepared and subjected to western blot analyses after immunoprecipitation with the anti-Flag polyclonal Ig. (**Upper**) Amounts of myc-tagged Navβ3 after immunoprecipitation detected by anti-myc antibody. (**Lower**) Amounts of input proteins, Flag-tagged Nav1.5 and myc-tagged Navβ3, detected by anti-Flag and anti-myc antibodies, respectively. Positions of size markers are indicated at the right. WT, wild-type.

## Discussion

Arrhythmias can be caused by mutations in the genes for cardiac ion channels producing action potentials. In BrS, the inward sodium current ($I_{Na}$) is more frequently affected than the other currents such as calcium and potassium.[32] To date, more than 300 disease-causing *SCN5A* mutations have been reported, and have been detected in 11–28% of BrS patients.[11,32] On the other hand, the prevalence of BrS-causing mutations in the genes for modifier proteins of Nav1.5, including GPD1-L, Navβ1, Navβ3 and MOG1, is relatively low.[23,24,32] In the present study, we identified a novel *SCN3B* mutation, V110I, in 3 Japanese BrS patients. It affected the evolutionary conserved residue of Navβ3, not found in the control subjects, decreased the cell surface expression of Nav1.5, and impaired $I_{Na}$ function. These observations strongly suggested that the *SCN3B* mutation was a BrS-causing mutation. It is noteworthy that, among these 3 patients, 2 had family histories of arrhythmia and/or sudden cardiac death, while the family history was uncertain in the other patient, indicating that the *SCN3B* mutation was rare but could be found in a considerable proportion of *SCN5A*-negative BrS, especially familial cases; 2 in 19 (10.5%) familial cases and 1 in 159 (0.6%) sporadic cases. Although there were no traceable genetic relations among the proband patients carrying the same mutation, the V110I mutation might be a founder mutation. Further investigation of the *SCN3B* mutation in a large cohort of familial BrS cases is required to assess the ancestral origin of mutation.

The cell surface expression of Nav1.5 was significantly reduced in the presence of Navβ3-L10P or-V110I in transfected cells. Although the cytoplasmic trafficking defect of Nav1.5 is well known to be an underlying mechanism for cardiac channelopathies, including BrS,[20,33] involvement of modifier proteins in the cell surface expression of Nav1.5 is poorly understood.[34] A pore-forming subunit of the voltage-gated sodium channel in the sensory nervous and atrial myocardium, Nav1.8, is highly homologous to Nav1.5.[35] It was reported that an endoplasmic reticulum (ER) retention sequence, RRR, in the cytoplasmic loop I of Nav1.8 caused retention of Nav1.8 on the ER, and masking of the retaining signal by Navβ3 released Nav1.8 for trafficking to the cell surface.[36] Because the RRR sequence is conserved in the cytoplasmic loop I of Nav1.5, Navβ3 might alter Nav1.5 trafficking by masking its ER reten-

tion signal. However, immunofluorescence studies demonstrated cytoplasmic colocalization of Nav1.5 and Navβ3, even in the presence of *SCN3B* mutations. This, in turn, implied that the trafficking defect of Nav1.5 was not caused by impaired formation of the sodium channel complex but by retention of mutant Navβ3 in the ER.

To date, 5 different β-subunits of the sodium channel have been identified.[25,34] In cardiomyocytes, Navβ1 and Navβ3 are preferentially expressed and modulate the function of Nav1.5 through non-covalent binding.[25] the structure of the β-subunits is relatively simple; forming with an Ig loop at the extracellular N-terminal region, 1 transmembrane domain, and a small intracellular C-terminal domain. In this study, both the L10P and V110I mutations affected the peak current of $I_{Na}$ in transfected cells via an affect on the trafficking of Nav1.5 to the cell surface. The binding of Nav1.5 and Navβ3, however, was not affected by the *SCN3B* mutations, suggesting that the Ig loop might not be involved in the binding to Nav1.5. On the other hand, these mutations showed different effects on the recovery from inactivation, indicating the possibility that the modulation of Nav1.5 function by Navβ3 might be controlled at multiple steps. It is interesting to note that the L10P mutation is also reported in AF.[30] The underlying mechanism of AF is a reentrant circuit in atrial tissues, where electrical conduction is delayed.[4,37] In patients with inherited AF who carried the *SCN5A* mutation, the delayed conductance is predicted to be induced by a slower upstroke of the action potential because of the loss-of-function mutation in *SCN5A*.[4] As shown in **Figure 3E**, slower recovery from inactivation associated with the L10P mutation might partly contribute to the further delayed upstroke of the action potential by decreasing the fraction of channels enrolling in the subsequent depolarization. The difference in inactivation recovery might be related to the differences in arrhythmic phenotypes.

We revealed that the L10P mutation decreased peak sodium current density by 37.5%. On the other hand, Hu et al reported that the L10P mutation decreased the peak current density by 80%, and approximately 40% of the transfectants did not produce the current,[23] and Olsen et al showed that the L10P decreased the peak currents by approximately 50%.[30] The reasons for these functional differences might be related to the different experimental conditions, including cell lines, the ratio of vectors, the presence of Navβ1, and the chemical composition of the bath solution. These differences would complicate the understanding and comparing of functional alterations caused by the mutations.

In summary, we identified a *SCN3B* V110I mutation in 3 unrelated Japanese patients with BrS that impaired intracellular trafficking and affected the electrophysiological function of Nav1.5, a hallmark of BrS. This is the first replicating report demonstrating a *SCN3B* mutation as a disease gene for BrS.

## Acknowledgments

This work was supported in part by Grant-in-Aids for Scientific Research from the Ministry of Education, Culture, Sports, Science and Technology, Japan; a Health and Labor Sciences Research Grant from the Ministry of Health, Labour and Welfare, Japan; grants for Basic Scientific Cooperation Program between Japan and Korea from the Japan Society for the Promotion of Science and the National Research Foundation, Korea, follow-up grants from the Tokyo Medical and Dental University, and Joint Usage/Research Program of Medical Research Institute Tokyo Medical and Dental University.

## Disclosures

Conflict of Interest: None declared.

## References

1. Brugada P, Brugada J. Right bundle branch block, persistent ST segment elevation and sudden cardiac death: A distinct clinical and electrocardiographic syndrome: A multicenter report. *J Am Coll Cardiol* 1992; **20:** 1391–1396.
2. Chen Q, Kirsch GE, Zhang D, Brugada R, Brugada J, Brugada P, et al. Genetic basis and molecular mechanism for idiopathic ventricular fibrillation. *Nature* 1998; **392:** 293–296.
3. Berne P, Brugada J. Brugada syndrome 2012. *Circ J* 2012; **76:** 1563–1571.
4. Amin AS, Tan HL, Wilde AA. Cardiac ion channels in health and disease. *Heart Rhythm* 2010; **7:** 117–126.
5. Schulze-Bahr E, Eckardt L, Breithardt G, Seidl K, Wichter T, Wolpert C, et al. Sodium channel gene (SCN5A) mutations in 44 index patients with Brugada syndrome: Different incidences in familial and sporadic disease. *Hum Mutat* 2003; **21:** 651–652.
6. Medeiros-Domingo A, Tan BH, Crotti L, Tester DJ, Eckhardt L, Cuoretti A, et al. Gain-of-function mutation S422L in the KCNJ8-encoded cardiac K(ATP) channel Kir6.1 as a pathogenic substrate for J-wave syndromes. *Heart Rhythm* 2010; **7:** 1466–1471.
7. Ueda K, Hirano Y, Higashiuesato Y, Aizawa Y, Hayashi T, Inagaki N, et al. Role of HCN4 channel in preventing ventricular arrhythmia. *J Hum Genet* 2009; **54:** 115–121.
8. Kattygnarath D, Maugenre S, Neyroud N, Balse E, Ichai C, Denjoy I, et al. MOG1: A new susceptibility gene for Brugada syndrome. *Circ Cardiovasc Genet* 2011; **4:** 261–268.
9. Burashnikov E, Pfeiffer R, Barajas-Martinez H, Delpon E, Hu D, Desai M, et al. Mutations in the cardiac L-type calcium channel associated with inherited J-wave syndromes and sudden cardiac death. *Heart Rhythm* 2010; **7:** 1872–1882.
10. Giudicessi JR, Ye D, Tester DJ, Crotti L, Mugione A, Nesterenko VV, et al. Transient outward current (I(to)) gain-of-function mutations in the KCND3-encoded Kv4.3 potassium channel and Brugada syndrome. *Heart Rhythm* 2011; **8:** 1024–1032.
11. Kapplinger JD, Tester DJ, Alders M, Benito B, Berthet M, Brugada J, et al. An international compendium of mutations in the SCN5A-encoded cardiac sodium channel in patients referred for Brugada syndrome genetic testing. *Heart Rhythm* 2010; **7:** 33–46.
12. Wilde AA, Brugada R. Phenotypical manifestations of mutations in the genes encoding subunits of the cardiac sodium channel. *Circ Res* 2011; **108:** 884–897.
13. Hermida JS, Lemoine JL, Aoun FB, Jarry G, Rey JL, Quiret JC. Prevalence of the brugada syndrome in an apparently healthy population. *Am J Cardiol* 2000; **86:** 91–94.
14. Antzelevitch C, Brugada P, Borggrefe M, Brugada J, Brugada R, Corrado D, et al. Brugada syndrome: Report of the second consensus conference: Endorsed by the Heart Rhythm Society and the European Heart Rhythm Association. *Circulation* 2005; **111:** 659–670.
15. Miyasaka Y, Tsuji H, Yamada K, Tokunaga S, Saito D, Imuro Y, et al. Prevalence and mortality of the Brugada-type electrocardiogram in one city in Japan. *J Am Coll Cardiol* 2001; **38:** 771–774.
16. Abriel H. Cardiac sodium channel Na(v)1.5 and interacting proteins: Physiology and pathophysiology. *J Mol Cell Cardiol* 2010; **48:** 2–11.
17. Ashino S, Watanabe I, Kofune M, Nagashima K, Ohkubo K, Okumura Y, et al. Effects of quinidine on the action potential duration restitution property in the right ventricular outflow tract in patients with brugada syndrome. *Circ J* 2011; **75:** 2080–2086.
18. Makita N, Behr E, Shimizu W, Horie M, Sunami A, Crotti L, et al. The E1784K mutation in SCN5A is associated with mixed clinical phenotype of type 3 long QT syndrome. *J Clin Invest* 2008; **118:** 2219–2229.
19. Watanabe H, Nogami A, Ohkubo K, Kawata H, Hayashi Y, Ishikawa T, et al. Electrocardiographic characteristics and SCN5A mutations in idiopathic ventricular fibrillation associated with early repolarization. *Circ Arrhythm Electrophysiol* 2011; **4:** 874–881.
20. Ackerman MJ, Siu BL, Sturner WQ, Tester DJ, Valdivia CR, Makielski JC, et al. Postmortem molecular analysis of SCN5A defects in sudden infant death syndrome. *JAMA* 2001; **286:** 2264–2269.
21. Makiyama T, Akao M, Shizuta S, Doi T, Nishiyama K, Oka Y, et al. A novel SCN5A gain-of-function mutation M1875T associated with familial atrial fibrillation. *J Am Coll Cardiol* 2008; **52:** 1326–1334.
22. Watanabe H, Koopmann TT, Le Scouarnec S, Yang T, Ingram CR, Schott JJ, et al. Sodium channel beta1 subunit mutations associated with Brugada syndrome and cardiac conduction disease in humans. *J Clin Invest* 2008; **118:** 2260–2268.
23. Hu D, Barajas-Martinez H, Burashnikov E, Springer M, Wu Y, Varro A, et al. A mutation in the beta 3 subunit of the cardiac sodium channel associated with Brugada ECG phenotype. *Circ Cardiovasc Genet*

2009; **2:** 270–278.
24. London B, Michalec M, Mehdi H, Zhu X, Kerchner L, Sanyal S, et al. Mutation in glycerol-3-phosphate dehydrogenase 1 like gene (GPD1-L) decreases cardiac $Na^+$ current and causes inherited arrhythmias. *Circulation* 2007; **116:** 2260–2268.
25. Brackenbury WJ, Isom LL. Na channel beta subunits: Overachievers of the ion channel family. *Front Pharmacol* 2011; **2:** 53.
26. Fahmi AI, Patel M, Stevens EB, Fowden AL, John JE 3rd, Lee K, et al. The sodium channel beta-subunit SCN3b modulates the kinetics of SCN5a and is expressed heterogeneously in sheep heart. *J Physiol* 2001; **537:** 693–700.
27. Valdivia CR, Medeiros-Domingo A, Ye B, Shen WK, Algiers TJ, Ackerman MJ, et al. Loss-of-function mutation of the SCN3B-encoded sodium channel {beta}3 subunit associated with a case of idiopathic ventricular fibrillation. *Cardiovasc Res* 2010; **86:** 392–400.
28. Tan BH, Pundi KN, Van Norstrand DW, Valdivia CR, Tester DJ, Medeiros-Domingo A, et al. Sudden infant death syndrome-associated mutations in the sodium channel beta subunits. *Heart Rhythm* 2010; **7:** 771–778.
29. Wang P, Yang Q, Wu X, Yang Y, Shi L, Wang C, et al. Functional dominant-negative mutation of sodium channel subunit gene SCN3B associated with atrial fibrillation in a Chinese GeneID population. *Biochem Biophys Res Commun* 2010; **398:** 98–104.
30. Olesen MS, Jespersen T, Nielsen JB, Liang B, Moller DV, Hedley P, et al. Mutations in sodium channel beta-subunit SCN3B are associated with early-onset lone atrial fibrillation. *Cardiovasc Res* 2011; **89:** 786–793.
31. Abramoff M, Magelhaes P, Ram S. Processing with ImageJ. *Biophoton Int* 2004; **11:** 36–42.
32. Hedley PL, Jorgensen P, Schlamowitz S, Moolman-Smook J, Kanters JK, Corfield VA, et al. The genetic basis of Brugada syndrome: A mutation update. *Hum Mutat* 2009; **30:** 1256–1266.
33. Watanabe H, Darbar D, Kaiser DW, Jiramongkolchai K, Chopra S, Donahue BS, et al. Mutations in sodium channel beta1- and beta2-subunits associated with atrial fibrillation. *Circ Arrhythm Electrophysiol* 2009; **2:** 268–275.
34. Rook MB, Evers MM, Vos MA, Bierhuizen MF. Biology of cardiac sodium channel Nav1.5 expression. *Cardiovasc Res* 2012; **93:** 12–23.
35. Facer P, Punjabi PP, Abrari A, Kaba RA, Severs NJ, Chambers J, et al. Localisation of SCN10A gene product Na(v)1.8 and novel pain-related ion channels in human heart. *Int Heart J* 2011; **52:** 146–152.
36. Zhang ZN, Li Q, Liu C, Wang HB, Wang Q, Bao L. The voltage-gated Na+ channel Nav1.8 contains an ER-retention/retrieval signal antagonized by the beta3 subunit. *J Cell Sci* 2008; **121:** 3243–3252.
37. Burstein B, Nattel S. Atrial fibrosis: Mechanisms and clinical relevance in atrial fibrillation. *J Am Coll Cardiol* 2008; **51:** 802–809.

## Supplementary Files

**Supplementary File 1**

**Table S1.** Nucleotide Sequences of Primers Used for Mutational Analysis of the Other Known Brugada Syndrome Genes

**Table S2.** Nucleotide Sequences of Primers Used in the Mutational Analysis of *SCN3B*

**Table S3.** Nucleotide Sequences of Primers Used in the Construction of Nav$\beta$3 Constructs

Please find supplementary file(s);
http://dx.doi.org/10.1253/circj.CJ-12-0995

(34.5–82.3%). Among these cases, 92.3% had a stenosis of 50%, and 76.9% had stenosis >70%; and we found that the stenotic rate of the proximal segment of the ACA had a negative correlation to the acute angle the aorta.

Although these cases were clinically presented with chest pain or discomfort, only 13 cases had ECG changes. Among these 13 cases, 11 received invasive coronary angiography, 9 cases had coronary atherosclerosis and 7 cases had two vessel disease. There were 9 cases of RCA originated from the left coronary sinus with an interarterial course. Among these 9 cases, 6 cases had significant stenosis at the proximal segments of RCA; 2 cases had minor stenosis and one had insignificant stenosis. Whether this atherosclerosis has correlation to the abnormal anatomical structure of the ACA, causing tubelant flow and resulting in premature atherosclerosis has no conclusion at present [8].

In conclusion, the advancement of diagnostic technologies, such as this noninvasive modality of MDCT, has advanced into shorter examination time, lower radiation exposure and better resolution imaging; and additionally, the relatively low cost of CTA at this country, MDCT can be regarded as the first-line examination in patients with chest pain, especially in those with high risk ACA.

## References


[1] Ben-Or S, Bowdish ME, Sheridan BC, Mill MR. Congenital coronary anomalies. In: Runge MS, Stouffer GA, Patterson C, editors. Netter's Cardiology. 2nd ed. Philadelphia, USA: Saunders; 2010. p. 481–6.

[2] Ocal A, Kilci H, Altunkas F, et al. Successful percutaneous coronary angioplasty in a patient with anomalous origin of the right coronary artery from the left anterior descending artery. Int J Cardiol Jun 25 2008;127(2):e42–4.

[3] Boissier F, Coolen N, Nataf P, et al. Sudden death related to an anomalous origin of the right coronary artery. Ann Thorac Surg 2008;85:1077–9.

[4] Schmitt R, Froehner S, Brunn J, et al. Congenital anomalies of the coronary arteries:imaging with contrast-enhanced multidetected computed tomography. Eur J Radiol 2005;15:1110–21.

[5] Taylor AJ, Rogan KM, Virmani R. Sudden cardiac death associated with isolated congenital coronary artery anomalies. J Am Coll Cardiol 1992;20:640–7.

[6] Manghat NE, Morgan-Hugiles GJ, Marshall AJ, et al. Multidetector computed tomography: imaging congenital coronary artery anomalies in adults. Heart 2005;91:1515–22.

[7] Angelini P. Coronary artery anomalies—current clinical issues: definitions, classification, incidence, clinical relevance, and treatment guidelines. Tex Heart Inst J 2002;29:271–8.

[8] Rigatellig G, Gemelli M, Zamboni A, et al. Are coronary artery anomalies an accelerating factor for coronary atherosclerosis development? Angiology 2004;55(1):29–35.


0167-5273/$ – see front matter 
doi:10.1016/j.ijcard.2012.04.130

# A novel 5′ splice site mutation of *SCN5A* associated with Brugada syndrome resulting in multiple cryptic transcripts

Toshio Shimada [a], Kimie Ohkubo [b], Keisuke Abe [a], Ichiro Watanabe [b], Naomasa Makita [a,*]

[a] *Department of Molecular Pathophysiology, Graduate School of Biomedical Sciences, Nagasaki University, Nagasaki, Japan*
[b] *Department of Cardiology, Nihon University School of Medicine, Tokyo, Japan*

ARTICLE INFO

*Article history:*
Received 9 April 2012
Accepted 22 April 2012
Available online 26 May 2012

*Keywords:*
Brugada syndrome
*SCN5A*
Splicing
Mutation
Acceptor
Exon trapping

*Dear Editor,*

We present a novel *SCN5A* splice mutation that results in multiple cryptic transcripts in a family with Brugada syndrome (Fig. 1A). A 25-year-old male presented with an episode of syncope after breakfast. ECG on admission showed minor ST elevation on V1 (Fig. 1B), which was converted to coved-type after the administration of pilsicainide (Fig. 1C). Structural heart diseases were excluded. VF was not induced by the programmed electrical stimulation. His mother (II:2) had no spontaneous ST elevation (Fig. 1D), but his cousin (III:3) had died suddenly during the third decade of his life. Genetic screening revealed a novel 5′ splice site mutation of exon 26 of *SCN5A* (c.4438-1C>T) in the proband and his mother (Fig. 1E,F). No mutations were identified in *SCN1B* or *SCN3B*.

To investigate the *in vitro* outcomes of the 5′ splice site mutation, a 1.0 kb genomic DNA fragment encompassing exons 25 and 26 was subcloned into an exon trapping vector pSPL3 [1]. Plasmids were transfected into COS-7 cells, and the transcripts were analyzed by reverse-transcription (RT)-PCR. As shown in Fig. 2A, the WT plasmid produced a single 399 bp transcript, whereas the mutant plasmid generated multiple aberrant transcripts (1–3), 295, 395, and 1195 bp in length. Sequencing revealed that, in transcript 1, two cryptic splice sites in exons 25 and 26 were activated, resulting in a 100 bp deletion of exon 25 and a 4 bp deletion of exon 26. In transcript 2, a cryptic splice site in exon 26 was activated, resulting in a 4 bp deletion of exon 26. In transcript 3, introns 25 and 26 were retained and lacked 116 bp due to activation of novel cryptic splice sites in intron 26. Thus, transcript 3 resulted in the longest RNA (1195 bp). RT-PCR from the proband's leukocytes showed two bands corresponding to transcripts 1 and 2 (data not shown).

The ultimate effects of aberrant splicing are not easily predicted because premature stop codons created by frame shifts often trigger the nonsense-mediated mRNA decay (NMD) pathway that degrades suboptimal mRNA before translation [2]. If these transcripts evade NMD, these mutants would yield proteins with

* Corresponding author at: Department of Molecular Pathophysiology, Graduate School of Biomedical Sciences, Nagasaki University, 1-12-4 Sakamoto, 852-8523 Nagasaki, Japan. Tel.: +81 95 819 7031; fax: +81 95 819 7911.
*E-mail address:* makitan03@yahoo.co.jp (N. Makita).

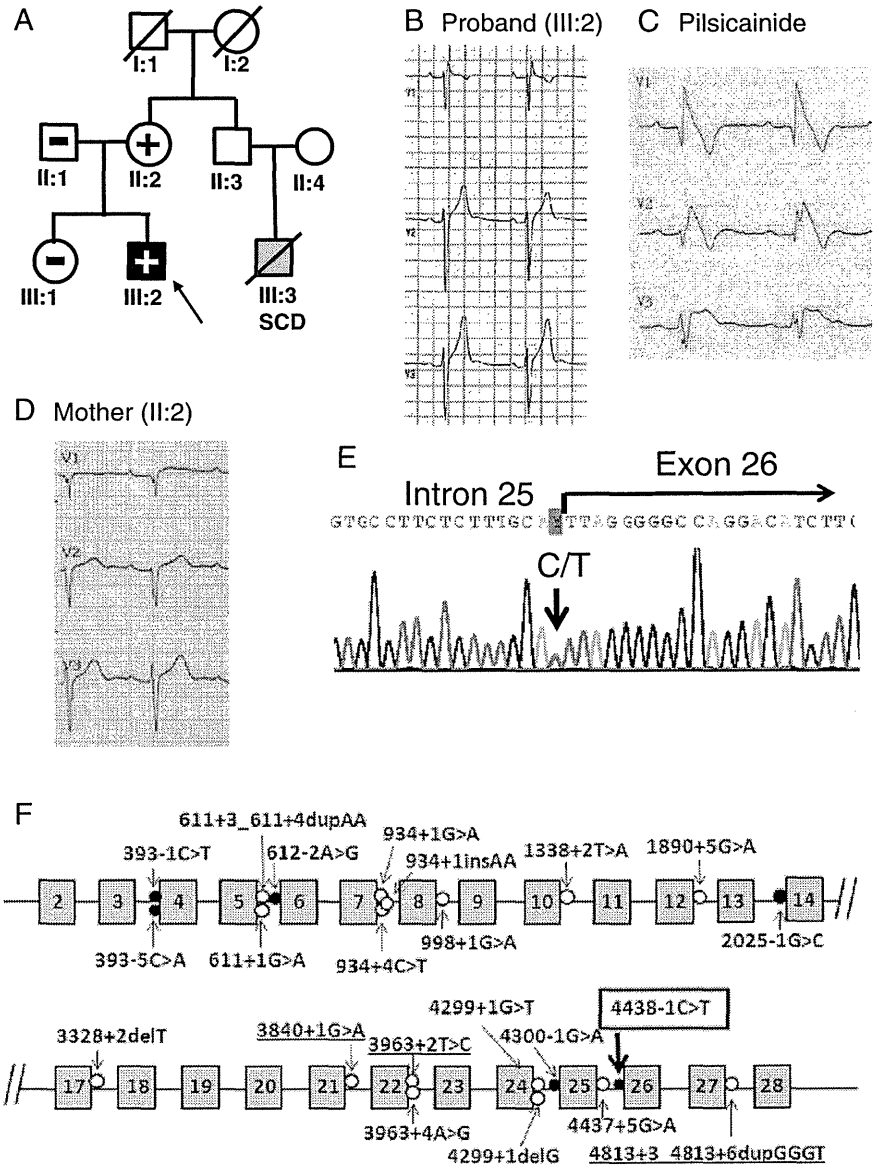


**Fig. 1.** Pedigree, ECG, and the DNA sequencing(A) The arrow indicates the proband. Closed, shaded, and open symbols show clinically affected, suspected, and genetically undetermined individuals, respectively. Plus and minus denote carriers and non-carriers of the mutation. SCD: sudden cardiac death. (B) A heterozygous mutation (C to T) at the 5′ splice site. ECG recordings of the proband (C, D) and mother (E). (F) Localization of *SCN5A* splice site mutations. Shaded boxes, open circles, and closed circles represent coding exons 2–28, mutations of 3′ and 5′ splice sites, respectively.

large truncations in the Na channel. For example, transcript 1 would change Tyr-1447 to Gly followed by 48 aberrant residues before a stop codon (Y1447GfsX48) (Fig. 2C). Similarly, transcripts 2 and 3 would result in L1480GfsX6 and L1480IfsX10, respectively. It is unlikely that these truncated channels would be functional.

Mutations in *SCN5A* account for 11–28% of the BrS probands [3]. A multicenter genetic study of 293 *SCN5A* mutations found that the vast majority of them (93%) were located at the coding exons, whereas 7% were at splice sites [4]. The functional consequences of coding mutations have been extensively studied using heterologous expression system. In contrast, among the 22 splice site mutations, *in vitro* consequences have been investigated in only three 3′ splice site mutations (underlined in Fig. 1F) and none of the 5′ splice site mutations [1,5,6].

Our study, for the first time, demonstrates the functional consequences of a 5′ splice site mutation of *SCN5A* responsible for BrS. The mutation results in multiple cryptic transcripts that potentially lead to large truncations of the Na channel. Despite sharing the same mutation, the mother is asymptomatic, lacking any obvious ECG abnormality. These findings confirm the notion that BrS has a very low penetrance. They also emphasize the importance of genetic testing of nonpenetrant mutation carriers and in family members of genotyped probands to detect early manifestation of the disease. Note, however, that, the presence of *SCN5A* by itself affects neither the carrier's prognosis nor the therapeutic strategies for BrS.

Supported by Grant-in-Aid for Scientific Research on Innovative Areas (HD physiology) 2213600 from the Ministry of Education, Culture, Sports, Science and Technology, Japan.

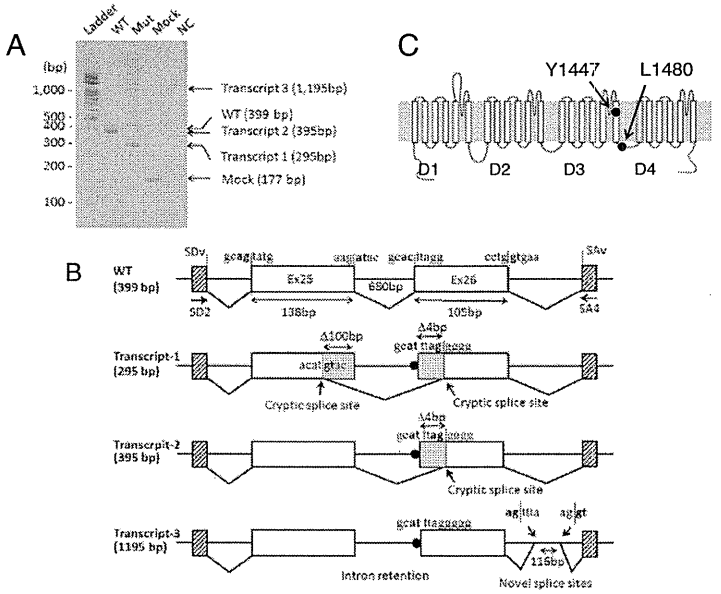


**Fig. 2.** Multiple aberrant *SCN5A* transcripts (A) Agarose gel electrophoresis of RT-PCR products from COS-7 cells transfected with a pSPL3 plasmid from either wild type (WT), mutant (Mut) fragment, or mock. NC: negative control. (B) Schematic representation of the splicing patterns of WT and mutant exon trapping plasmids. SDv and SAv represent vector splice sites, shaded boxes, and circles are the vector exons and the mutation, respectively. (C) Predicted locations of frame shifts in Nav1.5.

## References

[1] Rossenbacker T, Schollen E, Kuipéri C, et al. Unconventional intronic splice site mutation in SCN5A associates with cardiac sodium channelopathy. J Med Genet 2005;42:e29.
[2] Reed R, Hurt E. A Conserved mRNA Export Machinery Coupled to pre-mRNA Splicing. Cell 2002;108:523–31.
[3] Antzelevitch C, Brugada P, Borggrefe M, et al. Brugada syndrome: Report of the second consensus conference: Endorsed by the Heart Rhythm Society and the European Heart Rhythm Association. Circulation 2005;111:659–70.
[4] Kapplinger JD, Tester DJ, Alders M, et al. An international compendium of mutations in the SCN5A-encoded cardiac sodium channel in patients referred for Brugada syndrome genetic testing. Heart Rhythm 2010;7:33–46.
[5] Probst V, Kyndt F, Potet F, et al. Haploinsufficiency in combination with aging causes SCN5A-linked hereditary Lenegre disease. J Am Coll Cardiol 2003;41:643–52.
[6] Hong K, Guerchicoff A, Pollevick GD, et al. Cryptic 5' splice site activation in SCN5A associated with Brugada syndrome. J Mol Cell Cardiol 2005;38:555–60.

0167-5273/$ – see front matter 
doi:10.1016/j.ijcard.2012.04.114

Up-to-Date
Current Review

# 特発性心室細動と J波症候群の遺伝子診断

長崎大学大学院医歯薬学総合研究科分子病態生理学分野
教授 蒔田直昌
Naomasa Makita

## 特発性心室細動の定義

心室細動（ventricular fibrillation：VF）による突然死の症例は，冠動脈疾患・心筋症・弁膜症などの何らかの基礎心疾患を有することが多い．このような器質的心疾患や明白な心電図異常のないVF症例は，特発性心室細動（idiopathic ventricular fibrillation：IVF）と呼ばれる[1]．IVFは決して稀有な不整脈ではなく，若年者の突然死の約10%を占めるといわれ[2]，また約30%の症例はVFを再発する予後不良の不整脈である．唯一の有効な治療法は植込み除細動器（implantable Cardioverter Defibrillator：ICD）である[2]．一方，IVFの20%の症例に突然死の家族歴があることから[3]，少なくとも一部には遺伝的な要因の関与があると推測される[1, 2, 4]．したがって，IVFの遺伝子基盤を明らかにし，発症前から高リスクの家族を同定して，突然死の予防に役立てることは国民衛生上重要な課題である．しかし，IVFの患者には特徴的な心臓の構造異常や機能異常がないため，多くの単一遺伝子性の家族性不整脈と違って，突然死のリスクを持つ個人を発症前に同定するのはきわめて難しい．

IVFは，原因となる明白な基礎心疾患がないVFと定義されるため，その診断は基本的に除外診断である．歴史的には，先天性QT延長症候群，Brugada症候群，QT短縮症候群，カテコラミン感受性多形性心室頻拍などの致死性不整脈も，臨床的な特徴や電気生理学的な機序の詳細が明らかになる前はIVFと認識されていた．しかし，臨床検査法や遺伝子解析法の進歩とともにその実態が明らかになり，それぞれ独立した症候群として認識されている．このようにIVFの定義は，不整脈の臨床検査法や遺伝子解析技術の進歩とともに徐々に変化しており，画一的な線引きができないのが実情である．

## 早期再分極症候群 (early repolarization syndrome：ERS)

QRS-ST接合部（J点）の上昇は健常人にもしばしばみられる良性の心電図変化であると考えられてきた．歴史的にはGrantらが最初にこれを早期再分極（early repolarization：ER）と呼んだとされる[5]．J点の上昇は低体温の際に見られるOsborn波としてもよく知られている．Aizawaらは1993年，J波を伴うIVF症例を報告している[6]．HaïssaguerreらはIVF蘇生例206例を再検討したところ，31%に下方誘導または側方誘導に0.1mV以上のJ点の上昇がQRS直後のノッチやスラーとして認められたことから[7]，J波は必ずしも予後良好なバリエーションではなく，部位や広がりの程度によっては予後不良の予測因子と推測されている．

ERSは，早期再分極パターンを伴った心室細動症例と定義されるが，いくつかの変異の報告はあるものの，現時点で原因遺伝子として確定したものはない．$K_{ATP}$チャネルの一つKir6.1遺伝子（KCNJ8）に変異S422Lが同定され，その変異チャネルは$K_{ATP}$チャネルの機能を亢進させることが報告された[8]．しか

表　ERSとBrugada症候群の臨床的・遺伝学的特徴（文献12より改変）

| | ERS (Type I) | ERS (Type II) | ERS (Type III) | Brugada |
|---|---|---|---|---|
| 解剖学的部位 | 左室前側壁 | 左室下壁 | 左室・右室 | 右室 |
| J wave on ECG | I, V4-6 | II, III, aVF | 広範囲 | V1-V3 |
| 薬効 | | | | |
| Ic群 | ST/J：不変～＋/－ | ST/J：不変～＋/－ | ST/J：不変～＋/－ | ST/J：上昇 |
| キニジン | J正常化 | J正常化 | ? | J正常化 |
| イソプロテレノール | J正常化 | J正常化 | ? | J正常化 |
| 性差 | 男>>女 | 男>>女 | 男>>女 | 男>>女 |
| VF | 稀（健康男性や運動選手に散見） | Yes | Yes (Electrical Storm) | Yes |

し，Kir6.1は心筋での発現量が低いサブユニットであり，別の解析法ではS422Lの機能異常が追試できないことなどから，ERSの原因遺伝子としての妥当性に異論があった．最近，乳幼児突然死症候群（sudden infant death syndrome：SIDS）の遺伝子解析において，機能低下を示す2つのKCNJ8変異（E332del, V346I）が同定された．これらの報告を考慮すると，KCNJ8にはIVF関連遺伝子としての可能性が残されていると思われる[9]．しかし，前述のS422Lは機能亢進であるのに対して，E332del, V346Iは機能低下である．正反対の機能をもつ遺伝子変異を同一のレベルで議論し，IVFという一つの病態を理解するというのはきわめて困難である．また，KCNJ8のノックアウトマウスは冠攣縮性狭心症のモデルで，ST上昇と房室ブロックを伴って突然死することが知られている[10]．しかしそれがVFによる突然死かどうかは不明である．さらに，われわれも約30例のIVFで遺伝子解析したがKCNJ8の変異は同定されなかったことを考慮すると，KCNJ8変異はあったとしてもきわめてまれで，IVFの原因遺伝子であると断定するには議論の余地が多いと思われる．

一方，ERSとBrugada症候群には臨床的に類似した点が少なくないが，相違点も存在する．たとえばBrugada症候群では，Naチャネル遮断薬はBrugada型波形を増強または顕在化するが，ERSにおける効果は明らかではない．一方，$\beta$刺激薬やキニジンは両症候群に有効であり，また両症候群とも男性が多いことも類似した点である．また，Brugada症候群の中で下側壁誘導に早期再分極波形が不整脈発作の予後が予測因子であることも両症候群の関連を示唆するものである[11]．

Antzelevitchは最近，「J波症候群」という概念を提唱した[12]．Brugada症候群は右室の異常によって$V_{1\text{-}3}$でJ波が明らかになるのに対して，ERSは左室の前側壁や下壁で起きる異常によってI，$V_{4\text{-}6}$，II，III，aVFでJ波がみられる．しかし，これらはすべて共通したメカニズムを持つ「J波症候群」として扱うべきと主張するものである（表）．さらに彼らは，Brugada症候群とERSを合併する家系に，Caチャネルのサブユニット$\alpha$ 1C（CACNA1C），$\beta$ 2b（CACNB2b），$\alpha$ 2 $\delta$（CACN2D1）の遺伝子異常を報告し，両者にオーバーラップがあることも示唆している（図1）[13]．われわれも同様に，ERS患者の遺伝子解析によって3例のSCN5A変異を同定した（図2）[14]．これらはいずれもNaチャネルを無機能にする変異である．変異キャリアは，ピルジカイニド負荷によって下壁のJ波が増強しVFが誘発されたが，いわゆるBrugada型心電図パターンは示さなかった．これらの事実は，

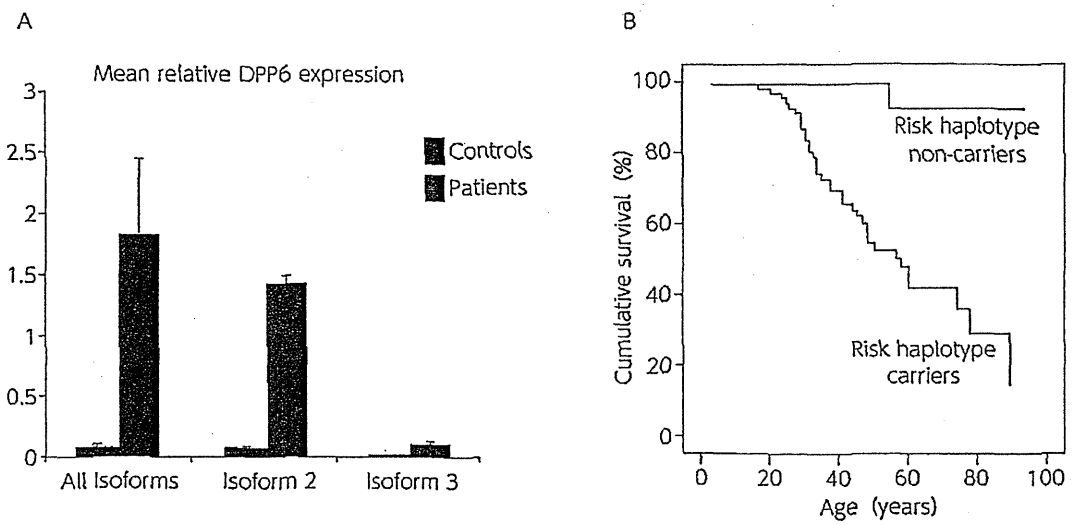


図3 IVF家系に認められたDPP6ハプロタイプの解析（文献15より改変）

A：心筋バイオプシーサンプルを用いて，3つのDPP6アイソフォームの発現レベルをRT-PCRで定量した．DPP6のハプロタイプを有するIVF患者心筋においてDPP6の発現は大きく亢進していた．

B：DPP6ハプロタイプのキャリアと非キャリアの生存曲線．キャリアの生存率は非キャリアに比べて明らかに低い．

このハプロタイプを持ちDPP6の発現量が亢進しているIVF患者ではそのような心電図異常が見られない．したがって現時点では，実際にDPP6の遺伝子異常がIVF患者における致死性不整脈の基質となっているとは断言できない．

また，心筋梗塞患者951人をVF群・非VF群に分け，ゲノムワイドで230万のSNP遺伝子タイピングを行うことによって，VFの関連遺伝子座が同定された[16]．この遺伝子座の近傍にはCoxsackievirus-adenovirus receptor (CXARD) がある．CXADRはコネキシン45とともに房室伝導をコントロールするタンパクであることが知られている．しかし現時点では，IVF症例にCXARD変異が同定されたという報告はない．

このように現時点では，KCNJ8, DPP6, CXARDのいずれもまだIVFの原因遺伝子として確立されたとはいえないが，今後，さらに次世代シークエンサーを用いたエクソーム解析が導入されれば，IVFの原因遺伝子の研究が急速に進む可能性があり，研究展開が注目される．

## 参考文献


1) Viskin, S. et al. Idiopathic ventricular fibrillation. Am Heart J. 120, 1990, 661-71.
2) Consensus Statement of the Joint Steering Committees of the Unexplained Cardiac Arrest Registry of Europe and of the Idiopathic Ventricular Fibrillation Registry of the United States. Survivors of Out-of-Hospital Cardiac Arrest With Apparently Normal Heart:Need for Definition and Standardized Clinical Evaluation. Circulation. 95, 1997, 265-72.
3) Haïssaguerre, M. et al. Mapping and ablation of idiopathic ventricular fibrillation. Circulation. 106, 2002, 962-7.
4) Noda, T. et al. Malignant entity of idiopathic ventricular fibrillation and polymorphic ventricular tachycardia initiated by premature extrasystoles originating from the right ventricular outflow tract. J Am Coll Cardiol. 46, 2005, 1288-94.
5) Grant, RP. et al. Spacial vector electrocardiography. The clinical characterisics of S-T and T vectors. Circulation. 3, 1951, 182-97.
6) Y. Aizawa. et al. Idiopathic ventricular fibrillation and

bradycardia-dependent intraventricular block. Am heart J. 1993, 126, 1473-4.
7) Haïssaguerre, M. et al. Sudden cardiac arrest associated with early repolarization. N Engl J Med. 358, 2008, 2016-23.
8) Medeiros-Domingo, A. et al. Gain-of-function mutation, S422L, in the KCNJ8-encoded cardiac KATP channel Kir6.1 as a pathogenic substrate for J-Wave syndromes. Heart Rhythm. 7, 2010, 1466-71.
9) Tester, DJ. et al. Loss-of-Function Mutations in the KCNJ8-Encoded Kir6.1 KATP Channel and Sudden Infant Death Syndrome/Clinical Perspective. Circulation. Cardiovascular Genetics. 4, 2011, 510-5.
10) Miki, T. et al. Mouse model of prinzmetal angina by disruption of the inward rectifier Kir6.1. Nat Med. 8, 2002, 466-72.
11) Kamakura, S. et al. Long-term prognosis of probands with Brugada-pattern ST-elevation in leads V1-V3. Circ Arrhythm Electrophysiol. 2, 2009, 495-503.
12) Antzelevitch, C. et al. J wave syndromes. Heart Rhythm. 7, 2010, 549-58.
13) Burashnikov, E. et al. Mutations in the cardiac L-type calcium channel associated with inherited J wave syndromes and sudden cardiac death. Heart Rhythm. 7, 2010, 1872-82.
14) Watanabe, H. et al. Electrocardiographic Characteristics and SCN5A Mutations in Idiopathic Ventricular Fibrillation Associated with Early Repolarization. Circulation : Arrhythmia and Electrophysiology. 4, 2011, 874-81.
15) Alders, M. et al. Haplotype-sharing analysis implicates chromosome 7q36 harboring DPP6 in familial idiopathic ventricular fibrillation. Am J Hum Genet. 84, 2009, 468-76.
16) Bezzina, CR. et al. Genome-wide association study identifies a susceptibility locus at 21q21 for ventricular fibrillation in acute myocardial infarction. Nat Genet. 42, 2010, 688-91.
17) Takehara, N. et al. A cardiac sodium channel mutation identified in Brugada syndrome associated with atrial standstill. J Intern Med. 255, 2004, 137-42.

# 早期再分極とJ波症候群：オーバービュー

時田直昌

長崎大学大学院医歯薬学総合研究科分子病態生理学

## ○ 早期再分極とJ波症候群

心電図QRS-ST接合部(J点)の上昇は健常人にもしばしばみられる変化であり，良性所見であると考えられてきた．歴史的には，Grantらが最初にこれを早期再分極(early repolarization；ER)と呼んだとされる[1]．一方，低体温の際にみられるいわゆるOsborn波のような顕著なJ波の増高は[2]，健常人に観察されることは稀である．このようなJ波の増高は，低体温時のみならず，低体温から回復後も遷延する場合があり，高Ca血症や特発性心室細動(idiopathic ventricular fibrillation；IVF)患者にもみられることがある．

この長らく良性の心電図所見と考えられていたJ点の上昇，すなわち早期再分極パターンは，最近の研究から，必ずしも良性とはいえないことが明らかになってきた．HaïssaguerreらはIVF蘇生例206例を再検討したところ，31%に下壁誘導または側壁誘導のQRS直後に0.1mV以上のJ点の上昇(ノッチやスラー)を認めた[3]．したがって，J波は必ずしも予後良好なバリエーションではなく，部位や広がりの程度によっては予後不良の予測因子と推測されている．

早期再分極症候群(*early repolarization syndrome*；ERS)は，下壁または側壁の少なくとも2つ以上の誘導に早期再分極パターン，すなわち0.1mV以上のJ点の上昇(QRS直後のノッチやスラー)を認めるIVFの1群と定義される．一方，Brugada症候群(Brugada syndrome；BrS)は，右側胸部誘導のcoved型・saddle back型ST上昇・J点上昇を特徴とするIVFの1群である．ERSとBrSには臨床的に類似点がある．例えば，J波はどちらの症候群においてもダイナミックに変化し，特に重症不整脈の出現時や直前に増高することが多い．また，β刺激薬やキニジンは両症候群に共通して有効であり，男性の罹患者が多いことも類似している．また，BrS患者の中で，下側壁誘導の早期再分極波形が不整脈発作の予後予測因子であるという事実も両症候群の関連を示唆している[4]．

Antzelevitchは最近，J波症候群(J wave syndromes)という概念を提唱した[5]．BrSは右室の異常によって$V_{1\sim3}$でJ波が明らかになるのに対して，ERSでは左室の前側壁や下壁で起きる異常によってI，$V_{4\sim6}$，II，III，$aV_F$でJ波がみられる．すなわち，J波の部位や臨床像に違いはあるものの，共通した機序を持つ広い疾患概念としてとらえることが提唱され，表1のように病型が分類された．側壁誘導に限局した早期再分極パターンはtype-1で，比較的若いスポーツ選手に多く，致死性不整脈のリスクは低い．一方，下壁，下側壁の誘導にみられる早期再分極パターンをtype-2と呼び，致死性不整脈のリスクは中等度である．それに対して，側壁，下壁，右側胸部誘導の広範囲のERパターンはtype-3と呼ばれ，ハイリスクグループであり，electrical stormをしばしば伴う．通常はtype-2の心電図だが，心室頻拍または心室細動(VT/VF)の直前に右側胸部誘導の著明なJ波増高を併発するものはtype-3に含まれる．一方，BrSは，右室胸部誘導に限局したJ波症候群の1型として分類されている．

## ○ Brugada症候群・早期再分極症候群の原因遺伝子

### 1. Brugada症候群

BrSにおけるST上昇の機序は，右室の心外膜に多く発現する一過性外向きK電流($I_{to}$)の相対的な増加

表1　早期再分極症候群とBrugada症候群の臨床的・遺伝学的特徴

| | ERS(Type Ⅰ) | ERS(Type Ⅱ) | ERS(Type Ⅲ) | Brugada |
|---|---|---|---|---|
| 解剖学的部位 | 左室前側壁 | 左室下壁 | 左室・右室 | 右室 |
| J波の部位 | Ⅰ, $V_{4\sim6}$ | Ⅱ, Ⅲ, $aV_F$ | 広範囲 | $V_{1\sim3}$ |
| 薬効 | | | | |
| Ic群 | ST/J：不変～+/− | ST/J：不変～+/− | ST/J：不変～+/− | ST/J：上昇 |
| キニジン | J正常化 | J正常化 | ? | J正常化 |
| ISP | J正常化 | J正常化 | ? | J正常化 |
| 性差 | 男>>女 | 男>>女 | 男>>女 | 男>>女 |
| VF | 稀(健康男性や運動選手に散見) | Yes | Yes(electrical storm) | Yes |

ISP：イソプロテレノール　　(文献5より改変引用)

表2　Brugada症候群と早期再分極症候群の原因遺伝子

| サブタイプ | 遺伝子 | 蛋白 | 遺伝子座 | 障害される電流 | 電流の効果 | 頻度 |
|---|---|---|---|---|---|---|
| A：Brugada症候群の原因遺伝子 | | | | | | |
| BrS1 | *SCN5A* | Nav1.5 | 3p21 | Na($I_{Na}$) | ↓ | 約20% |
| BrS2 | *GPD1L* | GPD1L | 3p22.3 | Na($I_{Na}$) | ↓ | 稀 |
| BrS3 | *CACNA1C* | Cav1.2 α1C | 12p13.3 | Ca($I_{Ca}$) | ↓ | 稀 |
| BrS4 | *CACNB2b* | Cav1.2 β2b | 10p12 | Ca($I_{Ca}$) | ↓ | 稀 |
| BrS5 | *SCN1B* | Navβ1 | 19q13.12 | Na($I_{Na}$) | ↓ | 稀 |
| BrS6 | *KCNE3* | MiRP2 | 11q13.4 | 一過性外向きK($I_{to}$) | ↑ | 稀 |
| BrS7 | *SCN3B* | Navβ3 | 11q24.1 | Na($I_{Na}$) | ↓ | 稀 |
| BrS8 | *KCNJ8* | Kir6.1 | 12p11.23 | K($IK_{ATP}$) | ↑ | 稀 |
| BrS9 | *CACNA2D1* | Cavα2d | 7q21.11 | Ca($I_{Ca}$) | ↓ | 稀 |
| BrS10 | *KCND3* | Kv4.3 | 1p13.2 | 一過性外向きK($I_{to}$) | ↑ | 稀 |
| BrS11 | *MOG1* | MOG1 | 17p13.1 | Na($I_{Na}$) | ↓ | 稀 |
| BrS12 | *ABCC9* | SUR2A | 12p12.1 | K($IK_{ATP}$) | ↑ | 稀 |
| B：早期再分極症候群の原因遺伝子 | | | | | | |
| ERS1 | *KCNJ8* | Kir6.1 | 12p11.23 | K($IK_{ATP}$) | | |
| ERS2 | *CACNA1C* | Cav1.2 α1C | 12p13.3 | Ca($I_{Ca}$) | | |
| ERS3 | *CACNB2b* | Cav1.2 β2b | 10p12 | Ca($I_{Ca}$) | | |
| ERS4 | *CACNA2D1* | Cavα2d | 7q21.11 | Ca($I_{Ca}$) | | |
| ERS5 | *ABCC9* | SUR2A | 12p12.1 | K($IK_{ATP}$) | | |
| ERS6 | *SCN5A* | Nav1.5 | 3p21 | Na($I_{Na}$) | | |

(文献7, 8より改変引用)

によって，活動電位第2相の貫壁性電位勾配が増大することであると考えられている[6]．1998年に，心筋Naチャネルαサブユニット遺伝子(*SCN5A*)変異が同定されて以降，これまでに300種近くの変異が報告され(BrS1)，そのほかにも11種類の原因遺伝子(BrS2～12)が知られている(表2)[7][8]．変異Naチャネルのほとんどは，ゲート機構の異常またはチャネル蛋白の細胞膜への輸送(membrane trafficking)によってNa電流量が減少または消失する(loss-of-function)．Na電流の抑制は，活動電位0相の急速な立ち上がりを抑制するとともに，それに引き続く1相の$I_{to}$を相対的に増加させる．

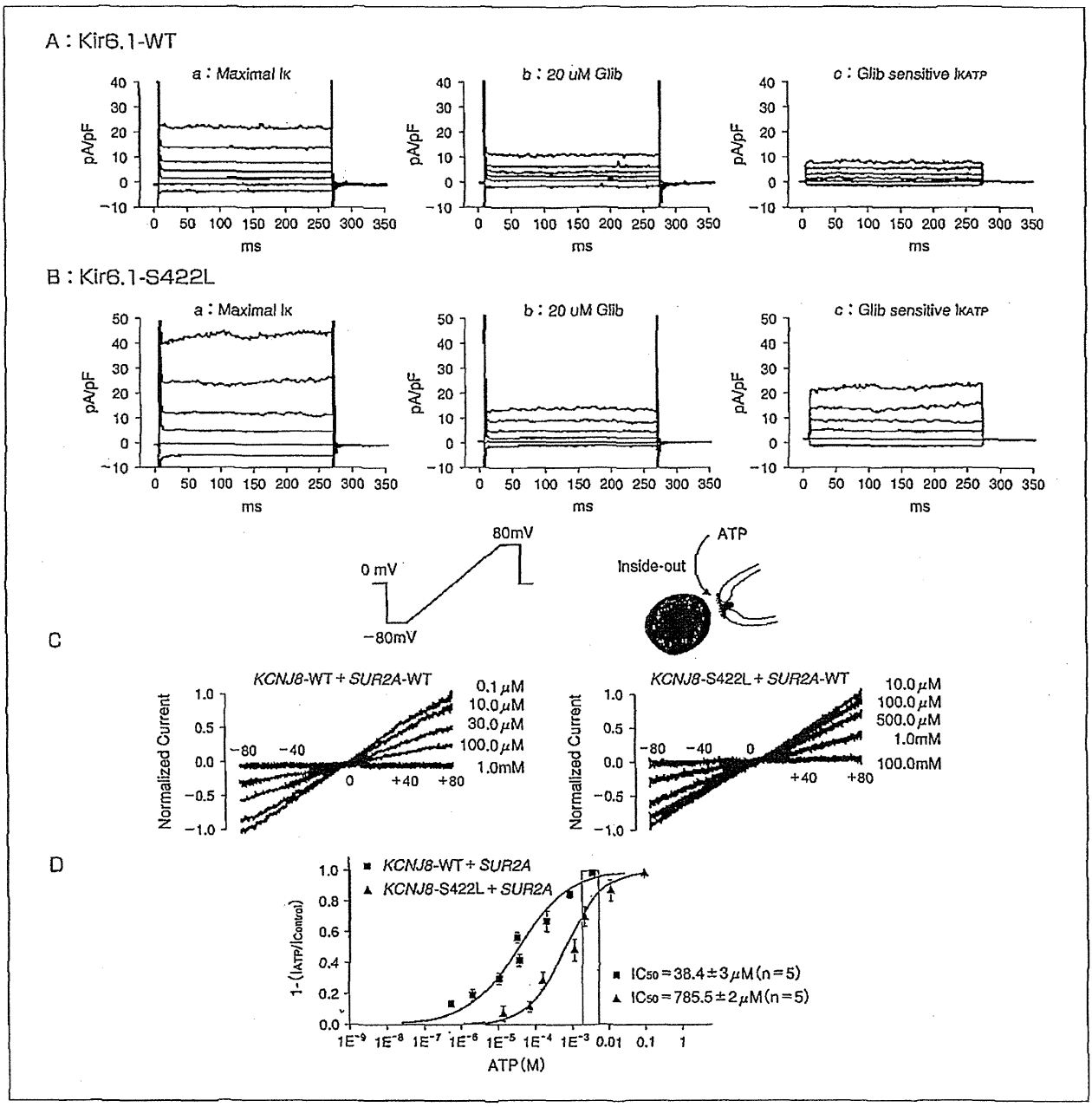


**図1　早期再分極症候群(ERS)に認められた*KCNJ8*変異S422Lの機能解析**

A, B：Kir6.1の野生型(WT)または変異S422LのプラスミドをSUR2AとともにCOS-1細胞で発現し全細胞K電流を測定した，100μMピナシジルで活性化した時(a)と，20μMグリベンクラマイドで抑制した時(b)の差分$K_{ATP}$電流(c)を示す．$K_{ATP}$電流の振幅はS422Lで増加している．

C, D：上記と同様な実験条件だが，細胞内をパッチの外側にして細胞内のATP量を変化させられるinside-out patch法を用いている．ランプパルスによって流れるK電流の振幅はATP濃度依存性に抑制されている．同一濃度のATPでWTとS422Lを比較すると，S422LではATPによる電流減少が抑制されて(すなわち電流量は増加して)いる．さらに，S422Lでは$IC_{50}$が約20倍上昇し，変異チャネルではATP感受性が低下していることを示している．

(文献21, 22より改変引用)

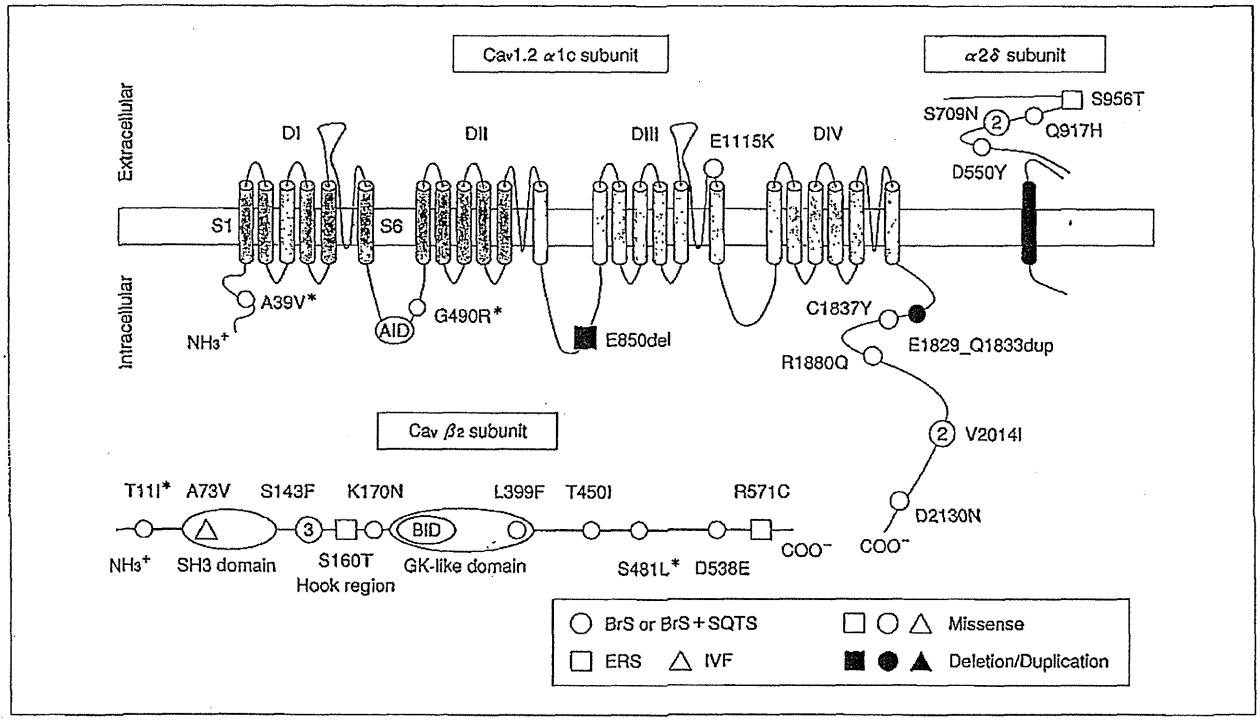


図2 ERS, IVF, Brugada症候群(BrS), QT短縮症候群(SQTS)に認められたCaチャネルの遺伝子変異
Cav1.2チャネルのα1cサブユニット, α2δサブユニット, β2サブユニットの変異が示されている. 同一遺伝子上の変異がみられることから, これらの不整脈が遺伝的にオーバーラップしているとわかる.
(文献18より改変引用)

*SCN5A*はBrS患者の最多の原因遺伝子(BrS1)であるが, 変異の検出率は約20%に過ぎない[8]. また, *SCN5A*陽性の家系内の中でも, 遺伝型と表現型が完全に一致しているわけではなく, 心電図異常のない*SCN5A*変異キャリアや, 典型的なBrugada型心電図を呈する非キャリアの存在する例も知られている[9]. 本症の突然死のリスク評価には, 失神などの症状, 突然死の家族歴, 電気生理学的心室細動誘発試験, 心房細動の有無, 加算平均心電図, $V_1$誘導のS波の幅などさまざまな要因が考慮されるが, *SCN5A*変異の有無は予後予測因子にはならない[10][11]. BrSの遺伝子解析の診断的意義は大きいが, リスク階層化を含む臨床的意義については, 少なくとも現時点では限定的である. *SCN5A*以外の遺伝子や未知の修飾遺伝子を含む「遺伝的背景」, 環境要因の関与を考慮する必要がある.

第2の原因遺伝子BrS2はglycerol-3 phosphate dehydrogenase like(*GPD1-L*)で[12], 変異蛋白はNaチャネルのトラフィッキングを阻害する[13]. QT短縮を合併したBrS家系にCaチャネル$\alpha_1$サブユニット(*CACNA1C*), $\beta_2$サブユニット(*CACNB2b*)の変異が報告されている[14]. また, 少数例ではあるが, 心筋Naチャネル$\beta_1$サブユニット(*SCN1B*)[15], $\beta_3$サブユニット(*SCN3B*)[16], Kチャネル*KCNE3*[17]が報告されている. さらに, Caチャネルα2δ・サブユニット(*CACNA2D1*)[18], ペースメーカーチャネル*HCN4*[19], *MOG1*[20]や, 後述するERSの関連遺伝子*KCNJ8*[21]にも変異が同定され, 関連遺伝子のリストはさらに拡大すると予想される.

## 2. 早期再分極症候群

これまでいくつかの孤発例や単一家系のERSで変異が報告されているものの, 現時点ではまだ確定的な原因遺伝子は知られていない. $K_{ATP}$チャネルの1

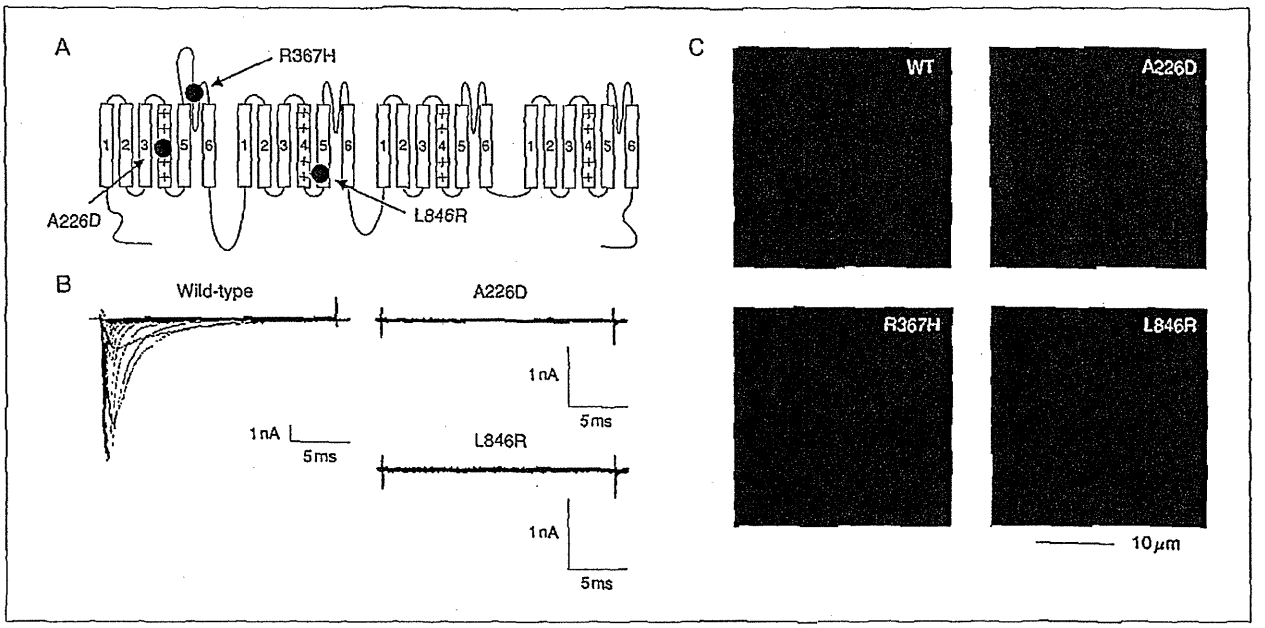


図3　IVF症例に同定された*SCN5A*変異

A：*SCN5A*の一次構造と3つのミスセンス変異の部位．6回膜貫通部位(S1-S6)を持つ4つのドメインがつながった形をしている．A226Dは電位感知S4セグメント，R367H，L846Rは中心孔を形成するS5-S6ループ，S5セグメントという，チャネルの基本構造として極めて重要な部位に存在する変異である．

B：細胞に発現させパッチクランプ法で解析すると，A226DとL846Rはいずれも無機能だった．R367Hは無機能であることを報告している．

C：NaチャネルにFLAGタグをつけて免疫染色し，共焦点レーザー顕微鏡で観察した各Naチャネルの細胞内局在．R367H，L846Rは野生型(WT)と同様に膜に存在していたが，A226Dは多くの蛋白が膜に達せずに細胞質内にとどまるトラフィッキング異常を示した．

(文献25，26より改変引用)

つKir6.1遺伝子(*KCNJ8*)に変異S422Lが同定され，その変異チャネルは$K_{ATP}$チャネルの機能を亢進させることが報告された(図1)[21][22]．しかし，Kir6.1は心筋での発現量が低いサブユニットである．また，上記の機能異常が別の解析法では追試できないことなどから，ERSの原因遺伝子としての妥当性に異論があった．最近，乳幼児突然死症候群(sudden infant death syndrome；SIDS)の遺伝子解析で，機能低下を示す2つの*KCNJ8*変異(E332del，V346I)が同定された．したがって，*KCNJ8*にはIVF関連遺伝子としての可能性が残されていると思われる[23]．しかし，前述のS422Lは機能亢進の変異であるのに対して，E332del，V346Iは機能低下である．正反対の機能をもつ遺伝子変異をIVFという1つの病態の理解に結びつけるのは極めて無理がある．また，*KCNJ8*のノックアウトマウスは冠攣縮性狭心症のモデルで，ST上昇と房室ブロックを伴って突然死することが知られている[24]．しかし，それがVFによる突然死かどうかはわからない．*KCNJ8*変異をERSの原因遺伝子と断定するには，議論の余地があると思われる．

BrSとERSの臨床的類似性についてはすでに述べたが，遺伝子レベルでもオーバーラップが認められる(表2)．BrSとERSを合併する家系に，Caチャネルのサブユニットα1C(*CACNA1C*)，β2b(*CACNB2b*)，α2δ(*CACN2D1*)の遺伝子異常が認められることが報告された(図2)[18]．われわれも同様に，ERS患者に3例の*SCN5A*変異を同定した(図3)[25]．これらはいずれもNaチャネルを無機能にする変異で，変異キャ